Suppression Method of Rising DC Voltage for the Halt Sequence of an Inverter in the Motor Regeneration

Jun-ichi Itoh, Wataru Aoki, Goh Teck Chiang, Akio Toba
Nagaoka University of Technology, Nagaoka Niigata, 940-2188 Japan
Fuji Electric Co. Ltd, Tokyo, Japan
itoh@vos.nagaokaut.ac.jp w_aoki@stn.nagaokaut.ac.jp tcgoh@vos.nagaokaut.ac.jp toba-akio@fujielectric.co.jp

Abstract— **In the power conversion system of electric vehicles, the inverter is shut down when the system fails in the cause of a drastic load change or other protection reasons. However, in the case if the inverter is shut down in regeneration mode, the DC link capacitor voltage is increased dramatically, which will potentially break the switching devices. In this paper, the authors propose a halt method to overcome the over voltage and over current problems in the case of system failure during the regeneration. The proposed method consists of two phases, in the phase I, the DC link capacitor voltage is controlled by charge and discharge switching patterns based on space vector of the inverter. Then, the phase II performs the short circuit operation in order to avoid the regenerating current from the motor flows into the DC link capacitor. The experimental results demonstrate that the DC link capacitor voltage is 80% lesser comparing to the conventional method. Furthermore, the circulating current can be suppressed by 46% from the proposed method.**

I. INTRODUCTION

Electric vehicles (EVs) have been remarkably research and studied, as the vehicle offers zero CO_2 commissions and high driving performance.

The power conversion system of the EVs has a different structure from a standard industrial motor drive system. In particular, the power conversion system connects a relay between the inverter and batteries for the purpose of system protection when the over voltage or over current occurs in the inverter due to system failure. In this case, the power between the inverter and the batteries is cutoff by the relay after cessation of normal operation. Then, the regeneration current is forced to flow into the DC link capacitor if the inverter is shut down in a way that all the switching devices are turned off at the same time. Consequently, the DC link capacitor voltage rises sharply in a short period because EV uses a small capacity such as film capacitor as the DC link capacitor. Electrolytic capacitor is often not applied due to the size minimization and high temperature operation condition. As a result, the switching device in the inverter will be broken when the DC link capacitor voltage becomes higher than the voltage rating of the switching devices.

One of conventional methods in order to solve this problem is connecting a brake chopper circuit in parallel to the DC link capacitor [1]. This method is known as the dynamic brake system which is typically applying in general purpose motor drive systems. When the DC link capacitor voltage exceeds the threshold voltage of the brake chopper, the regeneration power is consumed by the resistance in the chopper circuit. However, the dynamic brake system requires a switching device, a large electrolytic capacitor and a large-capacity resistance even it is only for the halt sequence during the system failures. The cost and volume of the dynamic brake system is not preferable in the power conversion system of EVs.

Several methods to reduce the volume of the dynamic brake system have been reported [2-3]. One of the methods is to use the dynamic brake system with the damping resistance. The proposed method utilizes the resistor in the dynamic brake system as the damping resistance element in the EV system. As a result, additional damping resistors are not required. Therefore, it can reduce the number of components. However, this method requires a large power capacity resistance.

A study also proposed that numbers of dynamic brake systems can be combined with just a switching device on the DC power supply wiring [3]. However, this method cannot be applied to the power conversion system of the EVs since only one inverter is used in a typical system.

In this paper, the halt sequence without the dynamic brake system is studied for EV system. Reference [4] shows a method to prevent the over voltage at the DC capacitor. This method proposes to short the terminal of

motor when the relay is cutoff during the regeneration mode. However, the inverter current increases dramatically during the operation results the over current occurs. Here, the authors proposed a method to utilize the relationship between the output voltage vector of the inverter and the electromotive force voltage of the motor during the regeneration in order to avoid the over voltage at the DC link capacitor, and also prevent the over current happening in the system. In addition, downsizing is possible because dynamic brake system is not required in the proposed method.

Firstly, the principle of the halt sequence method is discussed, and the problem of the conventional halt sequence that utilizes the vector control is described in this paper. Next, the proposed method using the space vector modulation is introduced. Finally, the effectiveness of the proposed method is confirmed in simulations and experimental results.

II. PRINCIPLES OF THE CONTROL METHOD

A. Over voltage problems in the halt sequence

Fig. 1 shows the system configuration of the power conversion system in EVs [6-5]. This system uses a two-level inverter in order to control an Interior Permanent Magnet Synchronous Machine (IPMSM). A small capacitance DC link capacitor C_{dc} is used to absorb the switching ripples. In addition, a relay is connected between the batteries and the inverter for the protection of the system.

Reference [4] shows the basic method to prevent the over voltage at the DC link capacitor, which intends to short the terminal of motor when the relay is cutoff. Both the upper and lower arms of the switches are turned on at the same time which can be known as the short-circuit mode. Then, the shorted arm is changing sequentially according to the phase voltage when only the zero-crossing currents are detected. From the operation, the current can be reduced to zero and the regenerative energy can be suppressed in a short period. However, this method has a problem that the large current (circulating current) flows inside the motor within the period of short circuit.

Here, the phenomenon of the current is considered during the short-circuit mode. Fig. 2 shows d-axis and q-axis equivalent circuits of the IPMSM without equivalent core-loss resistance [7]. Voltage equations are given by (1) and (2),

$$v_d = R_a i_d - \omega L_q i_q + \frac{di_d}{dt} L_d \qquad (1)$$

$$v_q = R_a i_q + \omega L_d i_d + \frac{di_q}{dt} L_q + \sqrt{3}\Psi_a \omega \qquad (2)$$

where L_d is the d-axis inductance, L_q is the q-axis inductance, ω is the angular velocity, Ψ_e is the linkage magnetic flux of armature by permanent magnet, i_d is the d-axis current and i_q is the q-axis current.

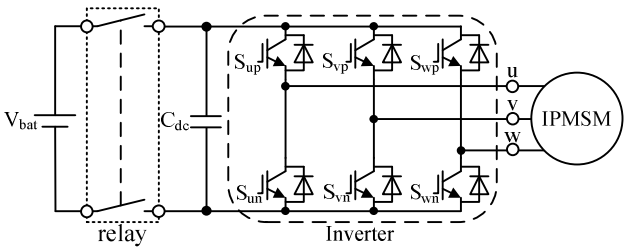

Fig.1. System configuration of adjustable speed drives with small capacitor in DC Link for EVs.

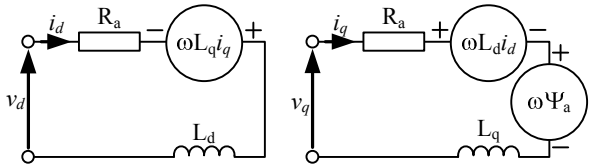

(a) d-axis equivalent circuit. (b) q-axis equivalent circuit.

Fig.2. d-axis and q-axis equivalent circuits of IPMSM.

Table1. Motor parameters of IPMSM

Rated Motor Power	5.5 kW
Rated Voltage	400 V_{rms}
Rated Current	10 A_{rms}
Rated Speed	1500 rpm
Number of Poles	6 poles
Winding Resistance	0.215 Ω
d-axis Inductance	4.3 mH
q-axis Inductance	10.2 mH

In addition, v_d and v_q are zero when the motor is shorted. Moreover, provided that the transient period is not considered then di_d/dt and di_q/dt are equal to zero. Under these conditions, voltage equation can be expressed by (3)

$$\begin{cases} -\omega L_q i_q + R_a i_d = 0 \\ R_a i_q + \omega L_d i_d = \sqrt{3}\Psi_a \omega \end{cases} \qquad (3)$$

d-axis and q-axis current are given by (4) and (5) from solving (3).

$$i_d = -\frac{\sqrt{3}\Psi_a \omega}{\frac{R_a^{\,2}}{\omega L_q} + \omega L_d} \qquad (4)$$

$$i_q = -\frac{\sqrt{3}\Psi_a \omega R_a}{R_a^{\,2} + \omega^2 L_d L_q} \qquad (5)$$

Finally, maximum oscillation current i_{amax} can be illustrated as (6).

$$i_{a\max} = \sqrt{i_d^{\,2} + i_q^{\,2}} \qquad (6)$$

From the above equation, it is possible that the maximum oscillation current during the short-circuit mode can be calculated from the motor parameters.

Table 1 shows the motor parameters of a IPMSM. The maximum oscillation current i_{amax} is 4.65 p.u. during the short-circuit mode. In order to confirm the validity of the expression, simulation is run under the same parameters. Fig. 3 shows output current waveform when the inverter turned into short-circuit mode during the halt operation. From the result, it is confirmed that the maximum oscillation current i_{amax} of steady state is 4.65 p.u., which is almost consistent to the calculated value.

EV Motor is typically designed in a matter that the maximum current is allowed up to 2.5 to 3.7 p.u. of the rated current [8-11]. Therefore, the motor can potentially suffer from damages during the short-circuit mode, considered that the circulating current is 4.65 p.u. of the rated current. Therefore, a method that can overcome the over voltage at DC link capacitor and also possible to keep low circulating currents are required.

B. Explanation of proposed method

The regeneration energy from the motor depends on the rotating speed and braking torque of the motor as (7).

$$\Delta W_\theta = -\int T \frac{d\theta}{dt} dt \qquad (7)$$

where θ is the rotation angle of the motor and T is torque of the IPMSM. In addition, the output torque of the IPMSM is given by (8).

$$T = P_n i_q \left\{ \sqrt{3}\Psi_e + \left(L_d - L_q\right) i_d \right\} \qquad (8)$$

where P_n is the number of the pairs of poles.

From (8), the negative torque will cause the increase of the DC voltage if the q-axis current is not controlled to zero. Thus, in order to prevent the over voltage at the DC link voltage, the q-axis current should be zero in the halt sequence immediately.

One of the strategies for the halt sequence, the current commands in the vector control should be zero before the inverter shuts down. However, this operation is depending on the current response of the regeneration current that is flowing into the DC link capacitor voltage.

Here, the proposed control method consists of two phases; in the phase I, the control ensures that the q-axis current equals to zero without a current regulator. The DC link voltage is controlled by selecting the switching patterns between the charge mode and discharge mode in the DC link capacitor (Switching patterns are illustrated in Table 2.). After the q-axis current becomes zero, the phase II is implemented in order to conduct the short-circuit mode until the d-axis current becomes zero.

In a matter of fact, the phase I alone can achieve the halt sequence and preventing the DC link capacitor from

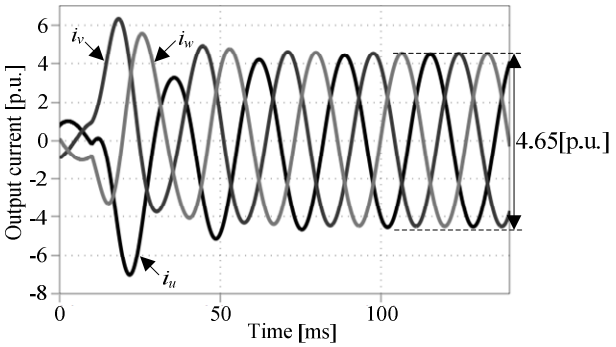

Fig. 3. Output current waveform with the short circuit control method.

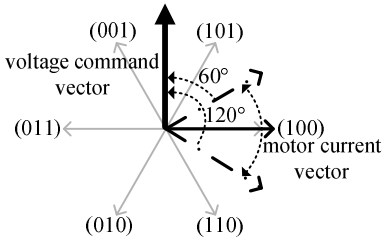

Fig. 4. Relationships between voltage command vector and vector of the motor current in phase I.

over voltage, since the motor currents are circulating in the inverter during the halt sequence. However, the motor current will be increased drastically in high speed region because of the electromotive force in the motor. As a result of the short circuit condition, the large motor current causes the irreversible flux loss in the magnet of the IPMSM. In addition, the inverter is required to implement with high current rating switching devices. Therefore, the phase I is introduced to prevent the occurrence of large motor current. By implementing the phase I, the maximum current in the halt sequence is suppressed to less than three times of the rating current of the motor. Note that the irreversible flux loss of the magnet does not occur in the IPMSM when the motor current is less than three times of the motor rating current generally.

Fig. 4 shows the relationship between the voltage command vector and the motor current vector in the phase I. The voltage command is 90 degrees ahead of the motor current vector. Therefore, the phase of the voltage command vector is controlled to a lead of 60 to 120 degrees with respects to the current vector of the motor. As a result, the q-axis current achieves zero at the very short time because the active current is changed into a reactive current.

However, the remaining regeneration energy is charged into the DC link capacitor because all of the active current cannot change quickly into the reactive current. Therefore, the proposed method includes a switching table to control the DC link capacitor voltage by charging and discharging the DC link capacitor during the phase I.

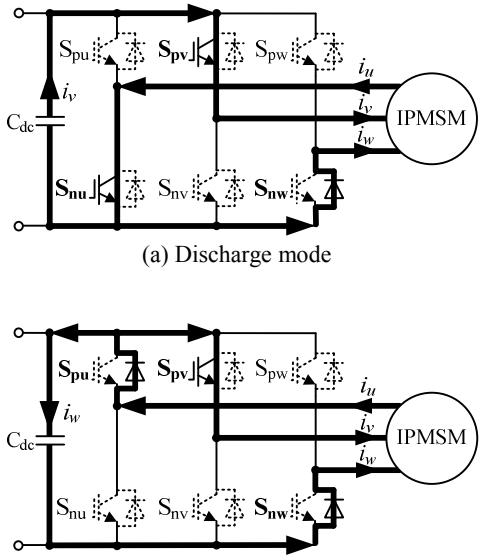

(a) Discharge mode

(b) Charge mode

Fig.5. Operational modes in phase I

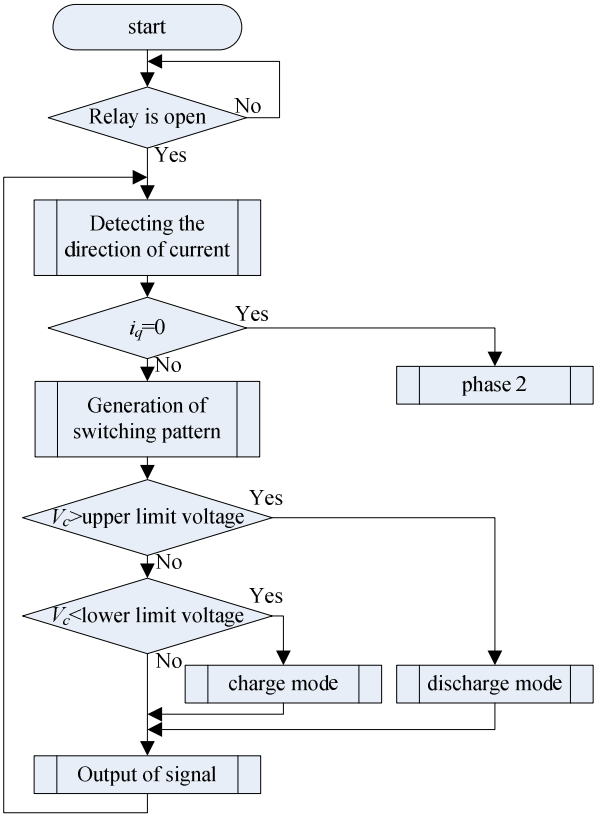

Fig. 6. Operation flow chart in phase I

Fig. 5 shows the equivalent circuit of the inverter in the phase I condition with the proposed method. Fig. 5(a) illustrates the discharge mode and Fig. 5(b) illustrates the pattern that against the current vector as set forth in Fig 5

Table 2. Switching table at phase I

	Direction of current			State of switch of inverter					
	i_u	i_v	i_w	S_{pu}	S_{pv}	S_{pw}	S_{nu}	S_{nv}	S_{nw}
discharge time	+	-	-	**ON**	OFF	**ON**	OFF	**ON**	OFF
	+	-	+	**ON**	OFF	OFF	OFF	**ON**	**ON**
	-	-	+	**ON**	**ON**	OFF	OFF	OFF	**ON**
	-	+	+	OFF	**ON**	OFF	**ON**	OFF	**ON**
	-	+	-	OFF	**ON**	**ON**	**ON**	OFF	OFF
	+	+	-	OFF	OFF	**ON**	**ON**	**ON**	OFF
charge time	+	-	-	OFF	OFF	**ON**	**ON**	**ON**	OFF
	+	-	+	**ON**	OFF	**ON**	OFF	**ON**	OFF
	-	-	+	**ON**	OFF	OFF	OFF	**ON**	**ON**
	-	+	+	**ON**	**ON**	OFF	OFF	OFF	**ON**
	-	+	-	OFF	**ON**	OFF	**ON**	OFF	**ON**
	+	+	-	OFF	**ON**	**ON**	**ON**	OFF	OFF

charge mode, respectively. These two operations are the fundamental switching patterns which are used to suppress the fluctuation of the DC link capacitor voltage. (The corresponding switching devices are changed according to the direction of motor current.)

Fig. 6 shows the operation flow chart in phase I. Once the relay is opened, the direction of the current is recorded then the q-axis current signal is comparing in the system to decide the operation between the phase I and phase . Then, the q-axis current is changed into reactive current by changing the voltage vectors in the inverter.

Table 2 illustrated the switching table that is implemented in the inverter that is depending on the capacitor voltage in subjects to the charge and discharge modes. The voltage command vector becomes a lead of 30-90 degrees with respects to the motor current vector during the discharge mode. Similarly, the voltage command vector becomes the lead of the phase of 90-150 degrees with respects to the motor current vector during the charge mode. As a result, the voltage command vector becomes the leading phase of 60-120 degree with respects to the motor current vector. The phase I operation ends when the q-axis current becomes zero.

Fig. 7 shows the short circuit operation mode that intends to prevent the DC link capacitor voltage from rising by circulating the regenerating current inside the inverter. In phase II, the switching states in the inverter create a short condition to prevent the DC link capacitor voltage from increasing. The following shows the switching states of the inverter, first, all of upper side arms (or lower side arms) of the inverter are opened as shown in Fig. 7(a). The switching state of Fig. 7(a) can avoid the motor current flows into the DC link capacitor because it is a short-circuit condition. Then, when the zero-crossing current is detected, the corresponded switch arm is opened sequentially as shown in Fig. 7(b), (Assuming that u-phase detects the zero-crossing). Thus, the inverter becomes a condition of a single phase operation. In addition, the torque is not produced in this state because the magnetic field of the stator becomes an alternating magnetic field.

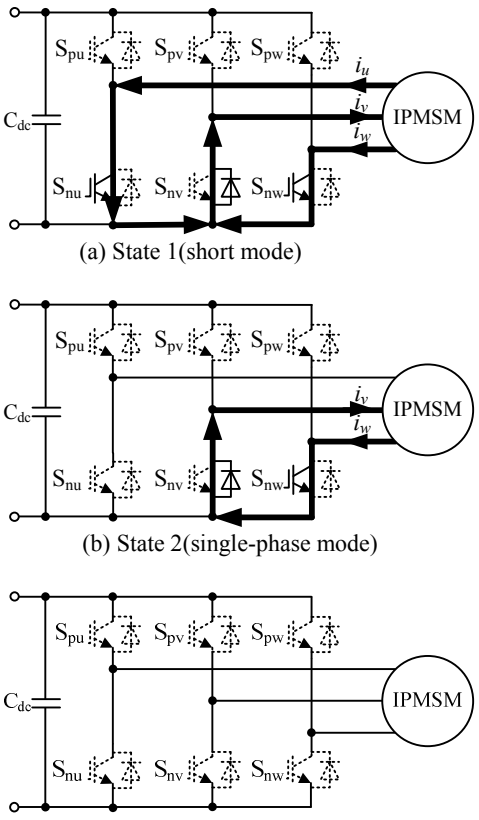

(a) State 1(short mode)

(b) State 2(single-phase mode)

(c) State 3 (all gate-off mode)

Fig. 7. Operational modes in phase II of the proposed halt sequence control method

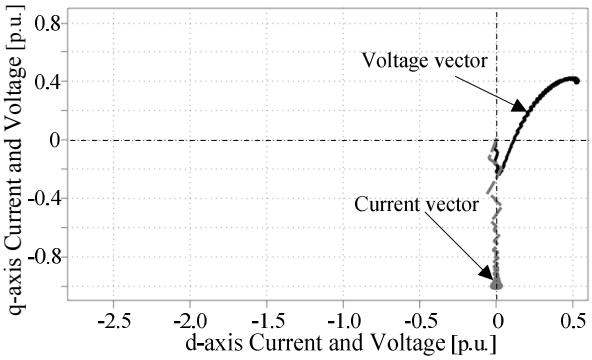

Fig. 8. Output voltage vector and output current vector in dq diagram. (Vector control is applied).

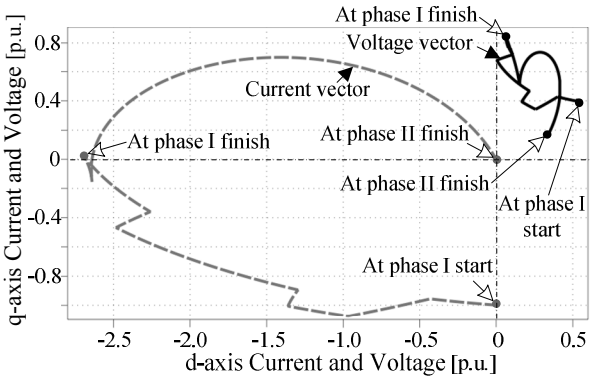

Fig. 9. Output voltage ve ctor and output current vector in dq diagram. (Proposed method is applied).

Finally, the remaining two switching arms are opened when the zero-crossing current are detected, respectively as shown in Fig. 7(c). Therefore, the suppression of the circulating current and the rising of the DC link capacitor voltage can be achieved.

C. The proposed method in a d-q diagram

Fig. 8 shows the relationships between the voltage vectors and current vectors in a d-q axis when the regenerative current is controlled by the vector control. In Fig.8, as soon the current vector is start moving, it can be noticed that the current vector is moving along the q-axis only. On the other hand, the voltage vector moves into the first quadrant as soon the control is started. Normally, the voltage vector is move to second quadrant in the motoring operation [12]. However, during the regenerating, the motor is working similarly as a generator, the voltage vector can be expressed by (9)

$$\dot{V}_{out} = \dot{V}_g - j\omega L_x \dot{I}_{out} \qquad (9)$$

where V_g is the induced EMF of the generator, L_x is synchronous reactance of the generator.

Fig. 9 shows the relationship between the voltage vector and current vector when the proposed method is applied. As shown in Fig. 9, the current vector is started at q-axis and ended at the d-axis when the phase I is completed. Then, the current vector moves back to the origin point from the fourth quadrant during the phase II. For the case of voltage vector, subjecting to the capacitor voltage condition, the voltage vector is moving towards the q-axis during the phase I, which is 90-120 degree subjecting to the current vector. As the phase 2 is started, the voltage vector is moving back to the origin point accordingly.

III. SIMULATION RESULTS

A. Verification of the proposed method

The IPMSM parameter that is shown in Table 1 is used in the simulation. The DC link capacitor voltage E_{dc} is 400 V and the capacity of the DC capacitor C_{dc} is 100μF. Fig. 10 shows the vector control with the propose method diagram [10].

Fig. 11 illustrates the waveform of the output current and the DC link capacitor voltage which are obtained by vector control only. Once the relay is opened at t_1, the q-axis command current is controlled to zero immediately. It can be note that the rising of DC link capacitor voltage is 76.4 V.

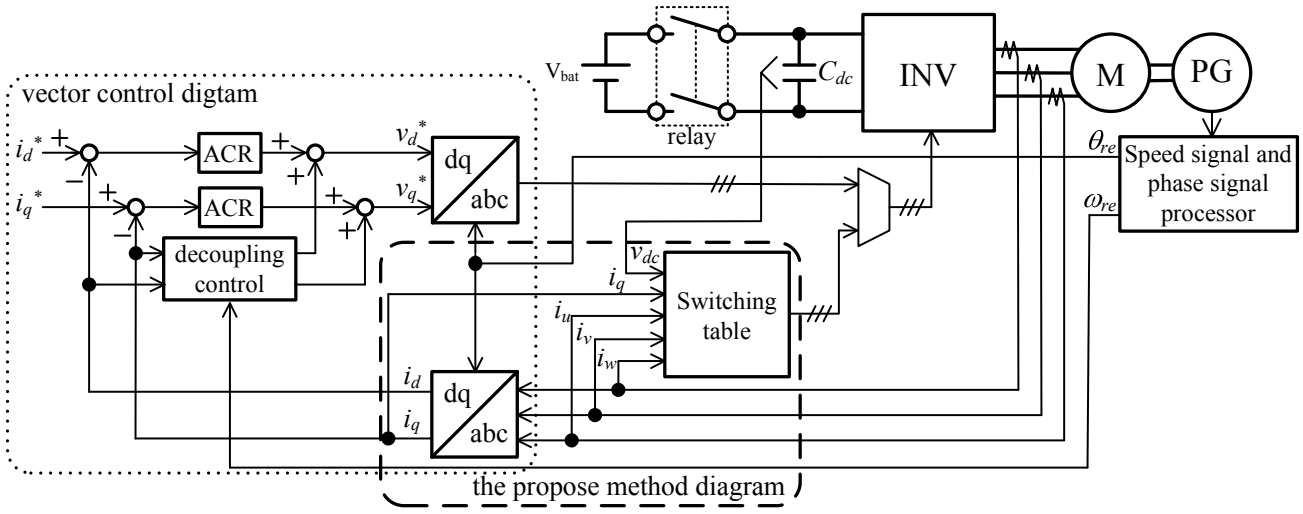

Fig. 10. vector control with the propose method diagram

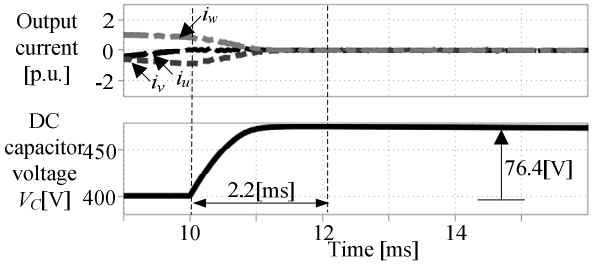

Fig. 11. Output current and DC capacitor voltage waveform without the proposed method

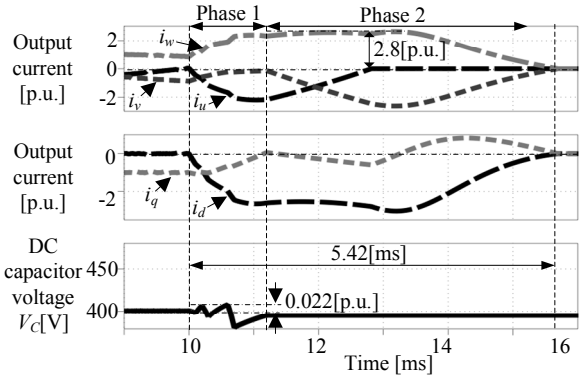

Fig. 12. Output current and DC capacitor voltage waveform with the halt sequence control method and countermeasure to current raised the recondition.

Fig. 12 shows the waveform of the output current and the DC link capacitor voltage which are obtained by the proposed method. In Fig. 10, once the relay is opened at 10 ms. Then, the switching patterns in Table 1 is implemented depending on the current polarity to ensure that the q-axis current equals to zero. At approximately 11 ms, the q-axis current reaches zero, then the phase II operation is implemented.

From the result, the output current can be suppressed to less than 2.80 p.u of the rated current by applying the proposed method. In addition, the fluctuation of the DC link capacitor voltage is suppressed to less than 0.022 p.u. of the rated voltage, which is sufficiently small.

B. Evaluation of IGBT Junction temperature

This section evaluates the junction temperature of the switching devices, considering that the proposed method is applied in an inverter with a 55 kW IPMSM. Table 3 shows the motor parameters. Table 4 shows the device parameters that are used in this section. The rated current for the selected device is approximately two times of the rated current of the motor. Considering that the heat capacity of the heatsink is large, therefore the heat resistance is not taken into accounts.

Fig. 13 shows simulation result of junction temperature for devices T_{Snu} T_{Snv} and T_{Snw}. In Fig. 13, the rise of temperature for IGBT T_{Snv} is approximately 9 degrees at highest and the rise of temperature for FWD T_{Snu} is 8.1 degrees at highest. From the results, it can notice that the change of temperature in IGBT is low for the implementation of proposed method. From the result, it can demonstrate that the implementation of the proposed method is not required high rated current devices, that is, the same rating devices that used in the conventional method can be applied. Furthermore, a large heatsink is not required since the change of temperature is relatively low.

IV. EXPERIMENTAL RESULTS

Fig. 14 shows the configuration of the experimental system. The parameters of the IPMSM are identical to the simulation condition as shown in Table 1. The DC link capacitor voltage E_{dc} is 200 V, the rated speed of IPMSM is 0.5 p.u. and a 7.5kW induction motor is used as the load machine. In addition, the halt sequence control is begun

Table 3. Motor parameters used in junction temperature simulations

Rated Motor Power	55 kW
Rated Voltage	400 V_{rms}
Rated Current	100 A_{rms}
Rated Speed	1500 rpm
Number of Poles	6 poles
Winding Resistance	0.0215 Ω
d-axis Inductance	0.43 mH
q-axis Inductance	1.02 mH

Table 4. inverter module parameters of inverter used in junction temperature simulations

Maximum Rated Collector-Emitter voltage		1200 V
Maximum Rated Collector current		100 A
Maximum Rated Junction temperature		448 K
Thermal resistance (1device)	Inverter IGBT	0.094 K/W
	Inverter FWD	0.150 K/W
Contact thermal resistance (1device)		0.0167 K/W

when DC link capacitor voltage E_{dc} is detected after the relay is opened.

Fig. 15 shows the experimental waveform of the output current and the DC link capacitor voltage which are obtained by vector control only. In Fig. 13(a), the DC link capacitor voltage is increased by approximately 110 V right after the relay is opened at t_1. After that, the dynamic break system is operated to ensure that the DC link capacitor voltage did not exceed the design value. As the energy is being consumed in the dynamic brake system, the DC link capacitor voltage drops immediately start from t_2.

Fig. 16 shows the experimental waveform of the output current and the DC link capacitor voltage which are obtained by the short circuit control method only. The maximum value of the circulating current is 4.6 p.u, which has been calculated from (6). However, for the safety purpose, the level of over current is set to 3.0 p.u. of the rated current. Therefore, in Fig. 16, the maximum value of the circulating current is shown as 3.0 p.u.. From the result, it is confirmed that this method is not practical because the DC link capacitor voltage rises sharply at this time. The reason is that increasing of the current causes the regenerative torque is increasing in the short circuit control method. Consequently, a large output current flows depending on the direction of the regeneration energy is increasing.

Fig. 17 shows the experimental waveform of the output current and the DC link capacitor voltage which are obtained by the proposed method. In Fig. 17(a), phase I is implemented between the time t_1 and t_2. During this period,

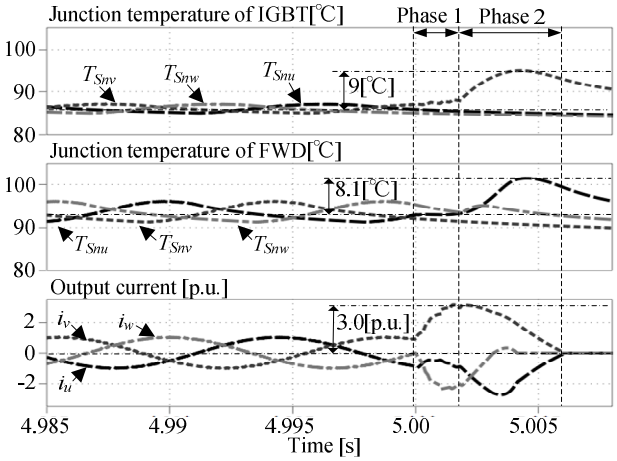

Fig. 13. Junction temperature waveform.

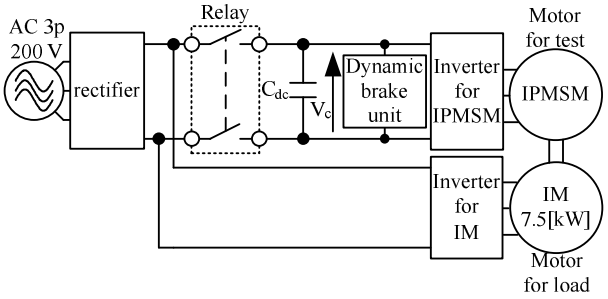

Fig. 14. Configuration of the experimental system.

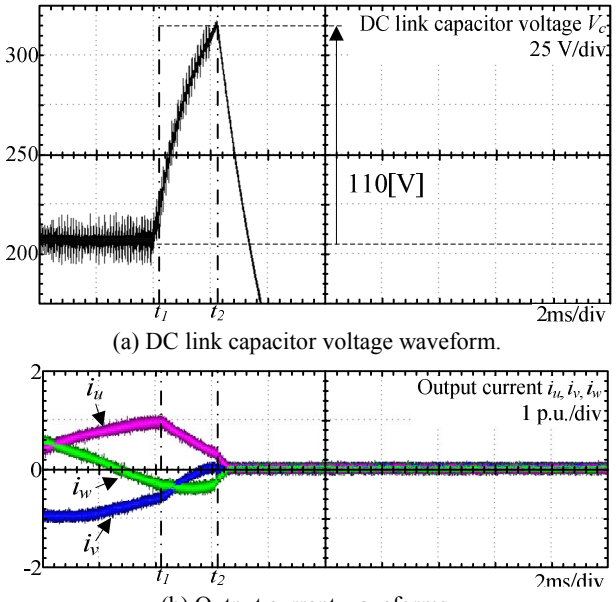

Fig. 15. Experimental result without the halt sequence control method.

it is confirmed that the DC link capacitor voltage fluctuates during from t_1 to t_2 as the switching patterns in Table 1 is applied. In addition, it is confirmed that the maximum capacitor voltage is 22 V during the phase I,

which is approximately 80% lesser comparing to the results in Fig. 15.

On the other hand, from Fig. 17(b), the maximum output current is 2.5 p.u., which is a 46% of suppression comparing to 4.6 p.u. as calculated early. From the experimental results, it is confirmed that without the dynamic brake system, the proposed method can prevent the over voltage happening at the DC link capacitor voltage, and also suppressing the circulating current.

IV. CONCLUSION

In this paper, the suppression method for the rising of the DC link voltage during the halt operation of the inverter while in the motor regeneration is proposed. The proposed method can stop the regeneration operation by utilizing the switching states of the inverter without the dynamic brake system. The simulation and experimental results demonstrate the effectiveness of the proposed method.

In the future works, the studies including the optimization of control of phase 1 and numerical analysis of the circulating current.

REFERENCES

[1] Jorge O. Estima and Antonio J. Marques Cardoso:" A Time-Coordination Approach for Regenerative Energy Saving in Multiaxis Motor-Drive Systems", IEEE Transactions on Power Electronis Vol. 27, No. 2, pp 931-941, (2012)

[2] K. Yamanaka, "Motor Control Device," JP Patent 2012-196143, July 20, 2012.

[3] S. Miyata, S, Takeuchi. "Motor Control," JP Patent 2000-188897, July 20, 2000.

[4] Jorge O. Estima and Antonio J. Marques Cardoso:" Efficiency Analysis of Drive Train Topologies Applied to Electric/Hybrid Vehicles", IEEE Transactions on Vehicular Techvology Vol. 61, No. 3, pp 1021-1031, (2012)

[5] Hui Zhang, Leon M. Tolbert and Burak Ozpineci:" Impact of SiC Devices on Hybrid Electric and Plug-In Hybrid Electric Vehicles", IEEE Transactions on Industry Application Vol. 47, No. 2, pp 912-921, (2011)

[6] W. Aoki, Y. Nakajima, J. Itoh and A. Toba: "Suppression method for the rise of DC voltage during the stop of inverter while in the motor regeneration" (in Japanese) , SPC-12-182, VT-12-033, HCA-12-067 (2012)

[7] S. Morimoto, Y. Tong, Y. Takeda and T. Hirasa." Loss minimization control of permanent magnet synchronous motor drives", IEEE Transactions on Industrial Electronics, Vol 41, NO. 5, pp 511-517, (1994)

[8] G. Pellegrino, A. Vagati, P. Guglielmi, and B. Boazzo: "Performance Comparison Between Surface-Mounted and Interior PM Motor Drives for Electric Vehicle Application" IEEE Transactions on Industrial Electronics, VOL. 59, NO. 2, pp 803-811, (2012)

[9] A. Nishio, M. Hirano, Y. Kato, T. Irie, T. Baba: "Development of Small Size, Light Weight and High Power IPM Motor for Electric Vehicle" Mitsubishi Heavy Industries, Ltd. Technical Review Vol.40 No.5, (2003)

[10] M. Terashima, T. Ashikaga, T. Mizuno, and K. Natori: "Novel motors and controllers for high-performance electric vehicle with four in-wheel motors", IEEE Trans. Ind. Electron., Vol. 44, No.2, pp. 28-38, (1997)

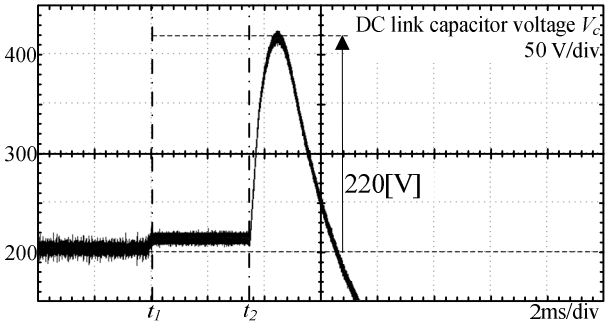

(a) DC link capacitor voltage waveform.

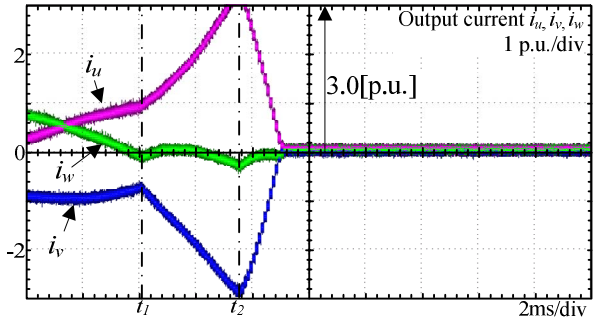

(b) Output current waveforms.

Fig. 16. Experimental result with the short circuit control method.

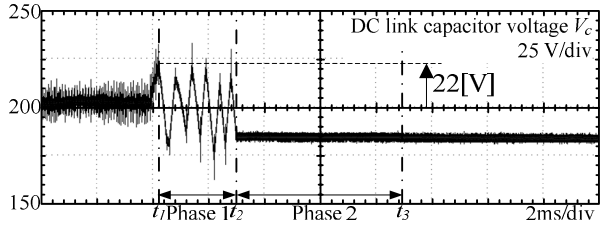

(a) DC link capacitor voltage waveform.

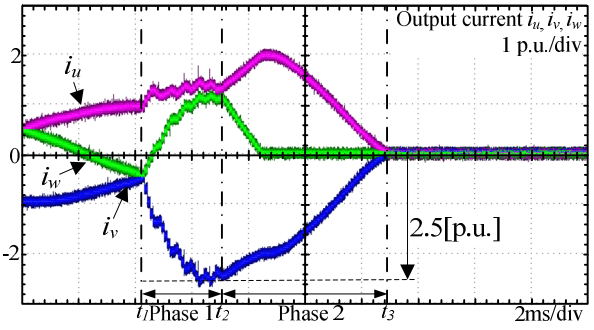

(b) Output current waveforms.

Fig. 17. Experimental result with the halt sequence control method.

[11] M. Terashima, et al.: "Drive System With 4 In-Wheel Motors for Electric Vehicle", 6th Annual Conference of IEEJ-IAS E. 3-7 (1992)

[12] J. Haruna and J. Itoh: "Modeling Design for a Matrix Converter with a Generator as Input," The Eleventh IEEE Workshop on Control and Modeling for Power Electronics (COMPEL 2008), COM352 (2008)